

Detection of Infrared Photons Using the Electronic Stress in Metal-Semiconductor Interfaces

P.G. Datskos^{a,b}, S. Rajic^a, C.M. Egert^a, and I. Datskou^c

^a Oak Ridge National Laboratory, P.O. Box 2008, Oak Ridge, TN 37831-8039

^b University of Tennessee, 401 Nielsen Physics Building, Knoxville, TN 37996-1200

^c Environmental Engineering Group, Inc., 11020 Solway School Rd, Knoxville, TN 37931-2052

ABSTRACT

It is well known that the work function of metals decreases when they are placed in a nonpolar liquid. A similar decrease occurs when the metal is placed into contact with a semiconductor forming a Schottky barrier. We report on a new method for detecting photons using the stress caused by photo-electrons emitted from a metal film surface in contact with a semiconductor microstructure. The photoelectrons diffuse into the microstructure and produce an electronic stress. The photon detection results from the measurement of the photo-induced bending of the microstructure. Internal photoemission has been used in the past to detect photons, however, in those cases the detection was accomplished by measuring the current due to photoelectrons and not due to electronic stress. Small changes in position (displacement) of microstructures are routinely measured in atomic force microscopy (AFM) where atomic imaging of surfaces relies on the measurement of small changes ($< 10^{-9}$ m) in the bending of microcantilevers. In the present work we studied the photon response of Si microcantilevers coated with a thin film of Pt. The Si microcantilevers were 500 nm thick and had a 30 nm layer of Pt. Photons with sufficient energies produce electrons from the platinum-silicon interface which diffuse into the Si and produce an electronic stress. Since the excess charge carriers cause the Si microcantilever to contract in length but not the Pt layer, the bimaterial microcantilever bends. In our present studies we used the optical detection technique to measure the photometric response of Pt-Si microcantilevers as a function of photon energy. The charge carriers responsible for the photo-induced stress in Si, were produced *via* internal photoemission using a diode laser with wavelength $\lambda = 1550$ nm.

Keywords: MEMS, micromechanical, photon detector, thermal detector, microcantilever, photo-induced stress, photoemission

1. INTRODUCTION

Photon detection and imaging has extensive medical, industrial, military, and commercial applications. The detection of infrared (IR) radiation, which is the second most intense radiation source in our environment, is very important for a variety of activities both commercial and military. Developing detectors that can sense electromagnetic radiation, especially in the far-infrared region (8 to 14 μm), allows the detection of unilluminated objects that are at room temperature. Presently, there are several families of available photon detectors, including a number of various solid state photon detectors¹. Photon detectors^{2,3} are in general classified as quantum detectors⁴ or thermal detectors such as pyroelectric⁵, thermoelectric, resistive

Further author information -

P.G.D. (Correspondence): E-mail: datskos@utk.edu; Telephone: (423) 574-6205; Fax: (423) 574-9407,

S.R.: E-mail: urv@ornl.gov; Telephone:(423) 574-6205; Fax: (423) 574-9407,

C.M.E. (deceased),

I.D.: Email: irene_datskou@cog-inc.com; Telephone:(423) 927-3717; Fax: (423) 927-3817

microbolometers,^{6, 7} and microcantilever thermal detectors.⁸⁻¹⁰ In photon detectors, incoming radiation is converted into electronic excitation; in thermal detectors, conversion of radiation into heat takes place, which is subsequently sensed as changes in the detector temperature. Among the various electromagnetic radiation detectors, the photon detector class has fast response times and high detectivities, D^* . Thermal detectors have a very broadband response, since they are based upon thermal conversion of the absorbed energy. Recently, a new type of thermal detector based on microcantilevers was developed⁹⁻¹⁰ with a reported⁹ $D^* \sim 10^8 \text{ cm Hz}^{1/2}\text{W}^{-1}$. More recently our group has developed a new approach for producing compact, light-weight, highly-sensitive micromechanical photon detectors that are based on MEMS (micro-electro-mechanical systems). It relies on the precise measurement of electronic stress produced due to internal photoemission in metal semiconductor micromechanical quantum detectors (MSMQD). When a MSMQD is exposed to photons (with energies above the Schottky barrier), the excess charge carriers generated induce an electronic stress, which causes the silicon microcantilever to deflect. This response is depicted schematically in Figure 1 for a MSMQD in the form of a microcantilever. Surface stresses s_1 and s_2 are balanced at equilibrium, generating a radial force F_r along the medial plane of the microcantilever. These stresses become unequal upon exposure to photons, producing a bending force, F_z , that displaces the tip of the microcantilever. Furthermore, since these MSMQDs are coated with a material that exhibits dissimilar thermal expansion properties than the semiconductor, the bimaterial effect will cause the device to bend in response to the electronic stress. The extent of bending is directly proportional to the radiation intensity.

Earlier work has shown that microcantilever bending can readily be determined by a number of means, including optical, capacitive, piezoresistive, and electron tunneling with extremely high sensitivity¹¹. For example, the metal-coated microcantilevers that are commonly employed in AFM allow sub-Angstrom ($<10^{-10}$ meter) sensitivity to be routinely obtained. For example, Hansma¹² and Binnig¹³ have demonstrated AFM sensitivities of 10^{-11} N, corresponding to bending magnitudes

reported. Microcantilevers can be mass produced at relatively low cost using standard semiconductor manufacturing methods. When microcantilevers are used as photon detectors and not as thermal detectors, they have faster response times and higher performance than that of microcantilever thermal detectors. Since microcantilevers can be easily manufactured in one- and two-dimensional arrays having 500 or more individual microcantilevers on a single wafer, this technology may be practical for manufacturing sensitive photon detector arrays with spatial resolutions comparable to current CCD detectors.

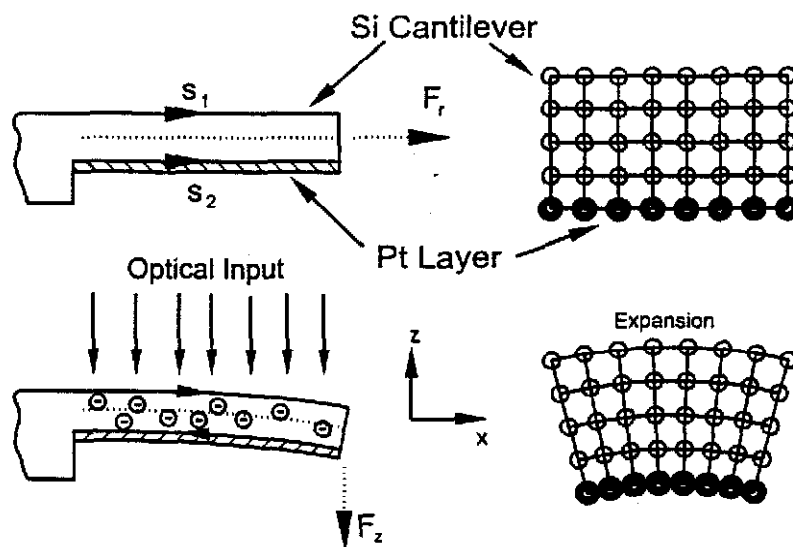


Figure 1. Schematic diagram showing the bending process of a MSMQD exposed to photons. Surface stresses s_1 and s_2 are balanced at equilibrium. Also depicted is the accompanied contraction of the semiconductor lattice following the injection of excess charge carriers.

2. METAL-SEMICONDUCTOR PHOTO-INDUCED ELECTRONIC STRESS

Microcantilevers (see Figure 1) undergo bending due to the differential surface stress ¹⁷ ($\Delta s = s_1 - s_2$) created by transient expansions; the top (photon exposed) side expands sooner than the bottom (unexposed) side thus creating a differential surface stress. Earlier work has shown that the absorption of photons by a solid results in temperature changes and thermal expansion which in turn gives rise to acoustic waves at frequencies corresponding to the amplitude modulation of the incident photon beam.^{18, 19} It was also demonstrated that the elastic wave stress amplitude can be larger than the radiation pressure amplitude.¹⁸ Acoustic signals that result from thermoelastic coupling have been used to obtain photoacoustic images of thin metallic films.⁹ It has been reported earlier that photoacoustic generation in semiconductors is due primarily to photogenerated charge carriers²⁰ and not to thermoelastic effects²¹; of course the energy of the incident photons has to be larger than the band gap energy of the semiconductor. It is well known that in a semiconductor the generation of "free" charge carriers (electrons and holes) via photon irradiation results in the development of a local mechanical strain.^{20, 22} This additional strain adds to other strains resulting from temperature changes of the semiconductor. When the photon flux is high enough to cause the semiconductor to heat, the subsequent expansion (or contraction) can be detected as acoustic waves with conventional photoacoustic techniques.^{19, 23}

In a semiconductor structure of thickness t and energy bandgap ϵ_g , the change in total surface stress due to a change in charge carriers, Δn , will be given by the photo-induced stress, Δs_{pi} , viz.^{20, 22, 24}

$$\Delta s = \Delta s_{pi} = \left(\frac{1}{3} \frac{d \epsilon_g}{d P} \Delta n \right) E \quad (1)$$

where, $d\epsilon_g/dP$ is the pressure dependence of the energy bandgap and E is the Young's modulus. A hole (in the valence band) decreases the energy of covalent bonds while an electron adds to the bonding (or antibonding) energy. Therefore there is a competing effect between the thermal and the photo-induced stress. When $d\epsilon_g/dP$ is negative, the photo-induced stress is of opposite sign than that of the thermal stress and will tend to make the semiconductor crystal contract.

For a rectangular bar (Figure 1) of length l , width w , and thickness t , the reciprocal of the radius of curvature, R , is given by Stoney's relationship²⁵

$$\frac{1}{R} = \frac{6(1-\nu)}{E t} \delta s_{pi} \quad (2)$$

where, ν is the Poisson's ratio. Using Eqn (1) the above equation can be rewritten as²⁴

$$\frac{1}{R} \approx \frac{2(1-\nu)}{t} \frac{d \epsilon_g}{d P} \Delta n \quad (3)$$

The reciprocal of the radius of curvature is approximately equal to d^2z/dy^2 .²⁶ Then the maximum displacement z_{max} of the microcantilever is given by

$$z_{max} \approx \frac{(1-\nu) l^2}{t} \frac{d \epsilon_g}{d P} \Delta n \quad (4)$$

The bending of a microstructure given by Eqn (4) is solely due to photo-induced surface stress. However, the overall change in z_{\max} will depend on several physical and mechanical properties of the metal/semiconductor system. Assuming that an incident radiant power, Φ_e , in a semiconductor microcantilever changes the number density, Δn , of excess charge carriers, we get

$$\Delta n = \eta \frac{\lambda}{hc} \frac{\tau_L}{l w t} \Phi_e^{abs} \quad (5)$$

where η is the quantum efficiency, h ($=6.625 \times 10^{-34}$ J s) is Planck's constant, c ($=3 \times 10^8$ m s⁻¹) is the speed of light, and τ_L is the lifetime of the carriers in the semiconductor. The quantum efficiency for a Schottky barrier can be described as³

$$\eta = C_0 \frac{(hc / \lambda - \Psi)^2}{hc / \lambda} = C_0 \frac{hc}{\lambda} \left(1 - \frac{\Psi \lambda}{hc}\right)^2 \quad (6)$$

where C_0 is in units of inverse energy and depends on the quantum yield and Ψ is the Schottky barrier height. Then the maximum displacement z_{\max} can be rewritten as

$$z_{\max} \approx C_0 \frac{(1-\nu) l^2}{t} \left(1 - \frac{\Psi \lambda}{hc}\right)^2 \frac{d \epsilon_g}{d P} \frac{1}{l w t} \tau_L \Phi_e \quad (7)$$

We can then define a deflection responsivity $\mathfrak{R} = z / \Phi_e$, viz.,

$$\mathfrak{R} = C_0 \frac{(1-\nu) l}{w t^2} \frac{d \epsilon_g}{d P} \left(1 - \frac{\lambda}{\lambda_c}\right)^2 \tau_L \quad (8)$$

where λ_c ($=hc/\Psi$) is the cutoff wavelength for photoemission from the Schottky interface.

Since the charge carriers can be generated in a very short time the photo-induced stress can manifest itself much faster than thermal stress. In the above treatment we ignored the thickness of the bimaterial layer. The bending, z_{\max} , of bimaterial microcantilevers caused by photoemission due to incident radiant power, Φ_e , can be written as²⁷

$$z_{\max} = C_0 \frac{l^2}{t_1 + t_2} \left[\frac{1 + (t_1 / t_2)^2}{3(1 + t_1 / t_2)^2 + (1 + t_1 E_1 / t_2 E_2) \left(\frac{t_1^2}{t_2^2} + \frac{t_2 E_2}{t_1 E_1} \right)} \right] \frac{E_1}{E^*} \frac{d \epsilon_g}{d P} \frac{\tau_L}{l w (t_1 + t_2)} \left(1 - \frac{\lambda}{\lambda_c}\right)^2 \Phi_e^{abs} \quad (9)$$

where t_1 and t_2 are the thickness of the bimaterial layer and microcantilever substrate, l is the microcantilever length, E_1 and E_2 are the Young's moduli of the bimaterial layer and microcantilever, and E^* is the effective Young's modulus of the coated microcantilever and is given by $E^* = E_1 E_2 / (E_1 + E_2)$. Materials with large differences in their Young's moduli will offer better

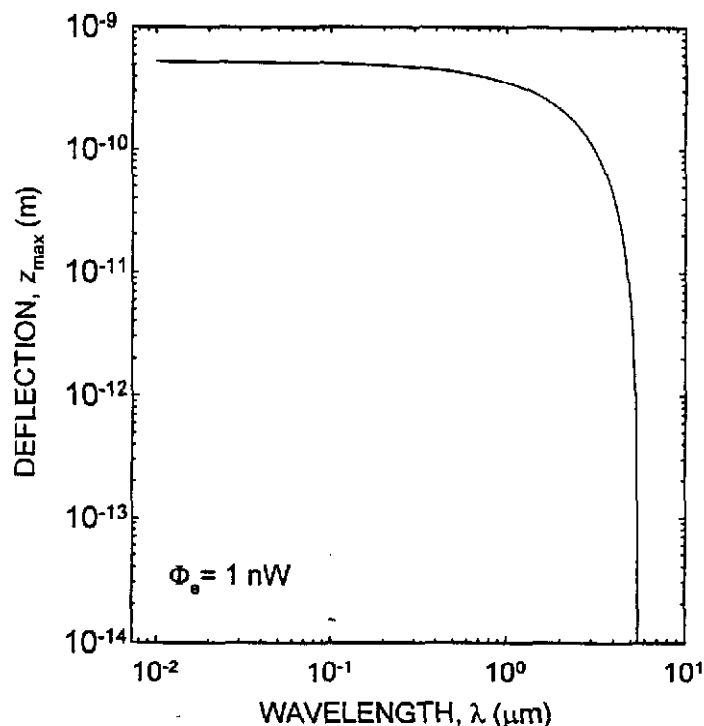


Figure 2. Calculated deflection of a Pt-Si quantum detector due to internal photo-emission stress as a function of photon wavelength for an absorbed power of 1 nW. The solid curve was calculated using Eqn (9).

deflection sensitivity. However, the larger the difference between the Young's moduli the more difficult it becomes to deposit a bimaterial layer and not produce "curled" microcantilevers.^{10, 15} The deposition of metal layers on thin microcantilevers to produce unstressed structures with no bending is difficult and requires extremely high thermal stability. Bimaterial microcantilevers with no noticeable bending have been produced when care was taken to avoid any temperature rises during the bimaterial deposition process.¹⁵ In those studies, the investigators broke down the complete deposition process into 20 steps in order to avoid the temperature of the microcantilever rising during the deposition.

Using values found in the literature²⁹ for Si ($de_g/dP = -2.9 \times 10^{-24} \text{ cm}^3$, and $E_I = 1.69 \times 10^{12} \text{ dyn/cm}^2$) and for Pt ($E_2 = 1.91 \times 10^{12} \text{ dyn/cm}^2$), we calculated from Eqn (9) the photo-induced deflection of a Pt-Si microcantilever photon detector as a function of photon wavelength; the absorbed power was assumed to be 1 nW. The Pt-Si microcantilever photon detector was given a length $l = 100 \text{ }\mu\text{m}$, width $w = 20 \text{ }\mu\text{m}$, thickness $t = 500 \text{ nm}$ and a 30 nm Pt coating. The overall bending due to internal photoemission is plotted in Figure 2 and can be seen to decrease with increasing wavelength up to the cutoff wavelength of PtSi ($\lambda_c = 5.5 \text{ }\mu\text{m}$),

3. EXPERIMENTAL

Although bending of micromechanical devices can readily be determined by a number of means (optical, capacitive, electron tunneling, and piezoresistive methods), in the present work we used optical readout techniques. The approach used was adapted from standard AFM imaging systems, and is shown schematically in Figure 3. Pt-Si microcantilevers were mounted on a three-axis translation stage to facilitate fine adjustment of the microcantilever relative to the rest of the experimental apparatus. Collimated optical radiation from a diode laser was used to evenly illuminate the mounted microcantilever (pump wavelength of 1550 nm, centered on the Pt-Si microcantilever, which had an effective length of 100 μm). A mechanical chopper was used to modulate the incoming photon radiation. This configuration provided a flexible, easily

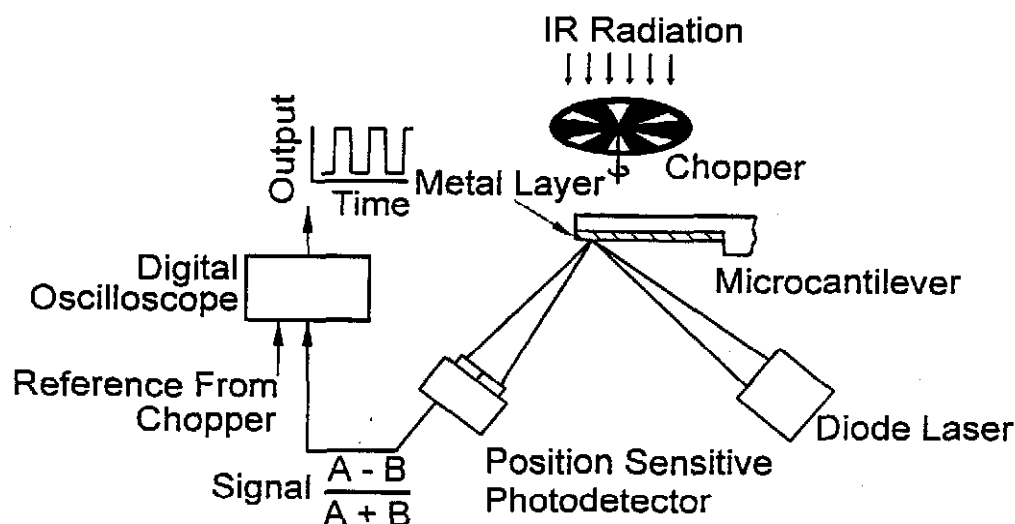


Figure 3. Schematic of the experimental setup and the optical readout scheme used in the present studies.

controlled test system for quantifying microcantilever response to optical energy. All measurements were conducted at ambient temperature and atmospheric conditions.

A second laser was used in a probe configuration to monitor bending. A 3 mW HeNe was focused onto the tip of the microcantilever using a 10 \times microscope objective; in order to minimize heating of the tip by the probe laser, the optical power was reduced by placing a neutral density filter with an optical density of 1.0 between the probe laser and the objective. A quad-element (A,B,C,D) photodiode detector was used to collect the reflected probe beam. The current output ($i_{A,B,C,D}$) of the photodiode depends linearly on the bending of the microcantilever. A high narrow bandpass optical filter is placed in front of the photodiode allowing the laser beam to be detected while preventing other wavelengths from reaching the photodiode. The amplified differential current signal from the quad cell photodiode, $i_{A,B,C,D} [(i_A+i_B) - (i_C+i_D) / (i_A+i_B + i_C+i_D)]$, is monitored and recorded using a digital oscilloscope (TDS 780, Tektronix) or sent to a lock-in amplifier (SR850, Stanford Research Systems) for signal extraction and averaging. Optical response characteristics of the 0.53 μm thick Pt-Si microcantilever was evaluated.

During our studies we fabricated platinum silicide by coating Si microcantilevers with a thin layer of Pt (30 nm). The microcantilevers were made from p-type Si. We used a broad argon ion beam and a Pt target to sputter a thin coating on one surface of Si microcantilevers. The coated devices were placed in a vacuum chamber and were heated to about 450 $^\circ$ C for a period of three to four hours to produce platinum silicide at the interface of Si and Pt. It is well known that initially Pt₂Si is formed and with additional time at the annealing temperature the conversion of Pt₂Si to PtSi occurs.³ In addition, the heating process helped reduce any residual mechanical stresses that were created as a result of the deposition process. This procedure seemed to result in microcantilever structure with almost no residual bending in the steady state. However, it is interesting to note that we observed that the resonance frequency of the Pt-Si microstructure was lower than the uncoated Si. It is rather difficult to say how much of the observed frequency shift was due to pure mass loading and how much due to residual stresses.

4. RESULTS AND DISCUSSION

Pt-Si microcantilevers were exposed to photons from a diode laser with wavelength $\lambda=1550$ nm and using a mechanical chopper, the incoming photon radiation was modulated at a frequency of 1120 Hz. Since Si is transparent to photons of wavelengths above 1100 nm, 1550 nm photons can reach the interface of Pt and Si and generate photoelectrons from platinum

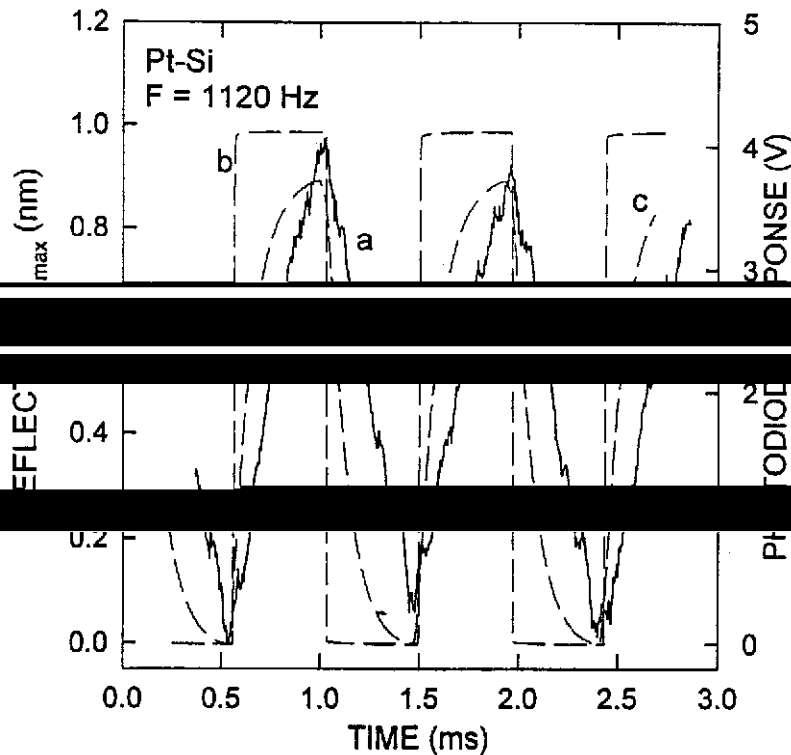


Figure 4. Deflection of a Pt-Si microcantilever [curve (a)] due to internal photoemission at the Pt-Si interface when exposed to photons with $\lambda=1550$ nm and an absorbed power of 20 nW. The dashed curves (b) and (c) go with the left vertical axis. The dashed curve (b) represents the signal from the modulator and shows the amount of time the Pt-Si microcantilever was exposed to photons. The dashed curve (c) is the signal from the quad cell photodiode and shows the time response of our optical position measuring circuit.

silicide. These electrons can drift into Si and cause an electronic stress. We measured the deflection of Pt-Si microcantilevers as a function of time and in Figure 4 plotted the temporal response when the absorbed optical power was 20 nW. The absorbed power was calculated using $\Phi_e^{abs} = \alpha_{abs} \Phi_e^{inc} A_{cant} / A_{spot}$ where α_{abs} (≈ 0.01) is the photon absorptivity of Pt at 1550 nm, A_{cant} is the cantilever area and A_{spot} ($= 1.75 \text{ mm}^2$) is the area of the focused laser beam at the plane of the microcantilever. As can be seen from Figure 4, the Pt-Si microcantilever responds rapidly to incoming photons that generate photoelectrons from the Pt-Si surface which, in turn, cause a measurable mechanical bending. For similar structures, thermal effects have been found to play a role in slower time scales with a time constants $> 10^{-3} \text{ s}$.²⁸ Since de_g/dP ($-2.9 \times 10^{-24} \text{ cm}^3$) is negative for Si²⁹, it excess electrons present in the Si will cause Si to contract while the Pt layer will either expand or remain unaffected. It is this bimaterial effect that makes the micromechanical structure to exhibit increased bending when exposed to infrared photons. We should point out that the temporal response of the Pt-Si microcantilever shown in Figure 4 (solid curve a) is limited by the time constant of optical read-out electronics. This observation is supported by the response of the read-out quad cell photodiode shown in Figure 4 (dashed curve c). It can be seen that the photodiode response is dramatically influenced by the time constant of the read-out circuit.

We also exposed our Pt-Si microcantilever to varying input radiant power and measured the microcantilever bending due to electronic stress as a function of absorbed power. Again, we calculated the absorbed power using $\Phi_e^{abs} = \alpha_{abs} \Phi_e^{inc} A_{cant} / A_{spot}$. In Figure 5 we plotted the measured bending of a Pt-Si microcantilever as a function of absorbed power using a diode laser source with wavelength $\lambda=1550$ nm. The deflection of the Pt-Si microcantilever was primarily due to electronic stress caused by internal photoemission and was found to increase linearly with increasing power with a deflection sensitivity $\mathfrak{R} = 0.0527 \text{ m/W}$. In our studies the smallest positional changes we measured were a fraction of a nanometer. However, much

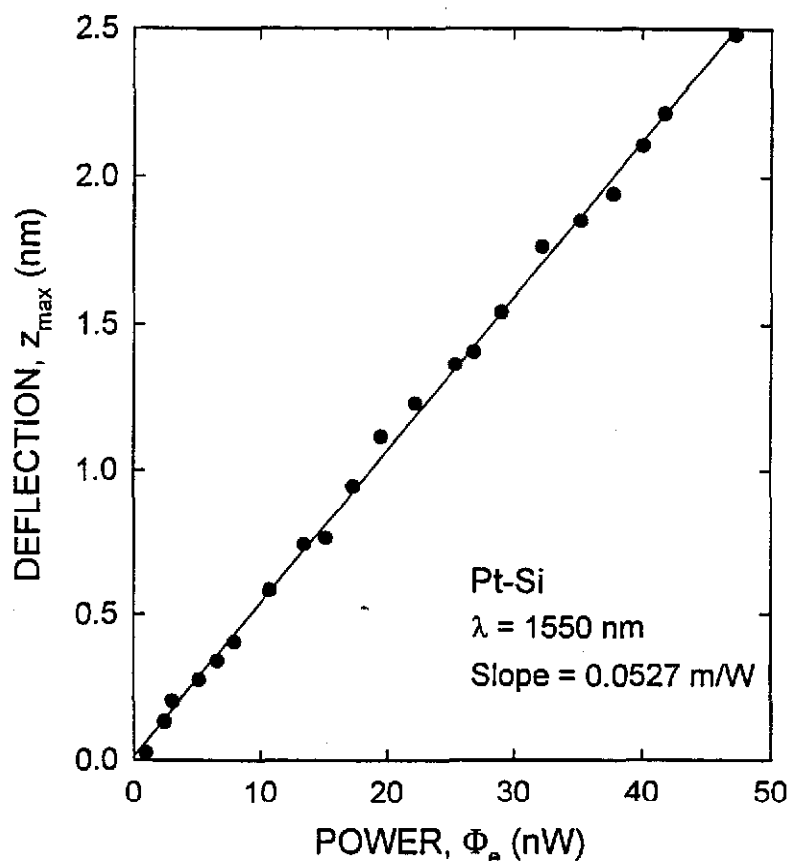


Figure 5. Deflection of a Pt-Si microcantilever as a function of absorbed power due to internal photo-emission when exposed to photons with $\lambda=1500$ nm.

smaller values are possible (10^{-12} m) corresponding to a minimum detectable power of 10^{-11} W which, in turn, translates to detectivity $D^* - 10^9$ cm $\text{Hz}^{1/2}\text{W}^{-1}$ at 30 Hz. This value is one order of magnitude higher than the D^* reported for microcantilever thermal detectors.⁹

Our results demonstrate that exposing Pt-Si microcantilevers to photons with energies above the PtSi Schottky barrier produces a photo-induced mechanical stress, which dominates over thermally-induced stresses. However, when the photon energy is below the PtSi Schottky barrier, thermal effects dominate. We found that the deflection of Pt-Si microcantilevers depend linearly on photoemissively-induced stress which, in turn, depends linearly on the input optical power and is manifested with fast response times. Furthermore, this mechanism does not rely on changes in the temperature of the microstructure and therefore thermal isolation (that is crucial to the operation of thermal detectors) has minimal influence. Utilizing such a detection mechanism, it may be possible to construct micromechanical photon detectors based on internal photoemission. Unlike thermal detectors that respond slowly (response times ~ ms) to impinging photons *via* temperature changes, a detector based on the photo-induced stress will respond both more sensitively and rapidly to incoming photons, with fast response times < ms.

An essential aspect of any scheme for micromechanical photon detection is the ability to sensitively detect physical changes resulting from photo-induced stress, since this directly affects the sensitivity and precision in measurement of photon flux. As an initial evaluation of the ability to detect optically-induced bending of a microstructure, Pt-Si microcantilevers were subjected to both mechanical and optical excitation, and their response measured as a function of excitation frequency. Mechanical excitation was achieved by driving a piezoelectric element with the reference signal from the lock-in amplifier; such a mechanical excitation response is helpful in locating resonance frequencies for allowed microcantilever bending (vibrational) modes.

5. CONCLUSIONS

The results of the present work demonstrate that Pt-Si microstructures represent an important development in micromechanical photon detector technology, and can be expected to provide the basis for considerable further development. For example, vastly improved micromechanical photon detectors could be produced by making relatively simple changes in the materials and geometries used in MEMS fabrication. It is possible to design microstructures with much smaller force constants by varying their geometry, and in contrast to the devices used in this study, microstructures with force constants as small as 0.008 N/m can be produced. Since the fundamental mechanical resonance frequency of a microstructure is proportional to the square root of the spring constant, $k^{1/2}$, reductions in force constant can be used to bring resonance into ranges compatible with mechanical chopping frequencies.

The micromechanical spectral response can be easily tailored through the application of specific antireflective coatings and choice of material for fabrication. This means that MEMS photon detectors can be fabricated using standard semiconductor methods and materials, and as a consequence could be mass produced at very low cost. Hence, two-dimensional cantilever arrays based on the technology described here, could become very attractive for a number of applications due to their inherent simplicity, high sensitivity, and rapid response to optical radiation. While the optical readout method is useful with single element designs, practical implementation of large micromechanical arrays may require the use of other readout methods, such as diffractive, piezoresistance or capacitance. Fortunately, the MEMS technology's compatibility with a variety of readout methods also affords tremendous flexibility to potential system designers.

ACKNOWLEDGEMENTS

The work performed by Oak Ridge National Laboratory was supported by DARPA, NSF and the Laboratory Director's Research and Development Program of Oak Ridge National Laboratory. The work performed by EEG, Inc. was supported by BMDO performed by EEG, Inc. was supported by BMDO under contract DASG60-98-M-0139. Oak Ridge National Laboratory is operated for the U.S. Department of Energy by Lockheed Martin Energy Research Corporation under contract DE-AC05-96OR22464.

REFERENCES

1. R. J. Kayes, *Optical and Infrared Detectors*, vol. 19. Berlin: Springer-Verlag, 1977.
2. J. L. Miller, *Principles of Infrared Technology*. New York: Van Nostrand Reinhold, 1994.
3. E. L. Dereniak and G. D. Boreman, *Infrared Detectors and Systems*. New York: Wiley and Sons, 1996.
4. A. Rogalski, "New Trends in Infrared Detector Technology," *Infrared Phys. Technol.* **35**, 1 (1994).
5. C. Hanson, "Uncooled Thermal Imaging at Texas Instruments," *Infrared Technology XXI, SPIE 2020*, 330 (1993).
6. R. A. Wood, "Uncooled Thermal Imaging with Monolithic Silicon Focal Planes," *Infrared Technology XXI, SPIE 2020*, 32 (1993).
7. P. W. Kruse, "Uncooled IR Focal Plane Arrays," *Infrared Technology XXI, SPIE 2552*, 556 (1995).
8. P. G. Datskos, P. I. Oden, T. Thundat, E. A. Wachter, R. J. Warmack, and S. R. Hunter, "Remote Infrared Detection Using Piezoresistive Microcantilevers," *Appl. Phys. Lett.* **69**, 2986 (1996).
9. E. A. Wachter, T. Thundat, P. G. Datskos, P. I. Oden, S. L. Sharp, and R. J. Warmack, "Remote Optical Detection Using Microcantilevers," *Rev. Sci. Instrum.* **67**, 3434 (1996).
10. R. Amantea, C. M. Knoedler, F. P. Pantuso, V. K. Patel, D. J. Sauer, and J. R. Tower, "An Uncooled IR Imager with 5 mK NEDT," presented at SPIE, Orlando, FL, 1997.
11. D. Sarid, *Scanning Force Microscopy*. New York: Oxford University Press, 1991.
12. J. H. Hoh, J. P. Cleveland, J.-P. Prater, and P. K. Hansma, "Quantized Adhesion Detected with Atomic Force Microscope," *J. Am. Chem. Soc.* **114**, 4917 (1992).
13. F. Ohnesorge and G. Binnig, "True Atomic Resolution by Atomic Force Microscopy Through Repulsive and Attractive Forces," *Science* **260**, 1451 (1993).

14. J. Varesi, J. Lai, T. Perazzo, Z. Shi, and A. Majumdar, "Photothermal Measurements at PicoWatt Resolution Using Uncooled Micro-Optomechanical Sensors," *Appl. Phys. Lett.* **71**, 306 (1997).
15. J. Lai, T. Perazzo, Z. Shi, and A. Majumdar, "Optimization and Performance of High-Resolution Micro-Optomechanical Thermal Sensors," *Sensors and Actuators* **58**, 113 (1997).
16. J. G. E. Harris, D. D. Awschalom, K. D. Maranowski, and A. C. Gossard, "Fabrication and Characterization of 100- μ m Thick GaAs Cantilevers," *Rev. Sci. Instrum.* **67**, 3591 (1996).
17. T. Thundat, P. I. Oden, P. G. Datskos, G. Y. Chen, and R. J. Warmack, "Microcantilever Sensors," presented at The 16th Warner Brandt Workshop on Charged Particle Penetration Phenomena, Oak Ridge Tennessee, 1996.
18. R. M. White, "Generation of Elastic Waves by Transient Surface Heating," *J. Appl. Phys.* **34**, 3559 (1963).
19. H. K. Wickramasinghe, R. C. Bray, V. Jipson, C. F. Quate, and J. R. Salcedo, "Photoacoustics on a Microscopic Scale," *Appl. Phys. Lett.* **33**, 923 (1978).
20. R. G. Stearns and G. S. Kino, "Effect of Electronic Strain on Photoacoustic Generation of Silicon," *Appl. Phys. Lett.* **47**, 1048 (1985).
21. A. Rosencwaig and M. White, "Imaging of Dopant Regions in Silicon with Thermal-Wave Electron Microscopy," *Appl. Phys. Lett.* **38**, 165 (1981).
22. T. Figielski, "Photostriction Effect in Germanium," *Phys. Status Solidi* **1**, 306 (1961).
23. P. Hess and A. C. Boccara, *Photoacoustic, Photothermal and Photochemical Processes at Surfaces and in Thin Films*. Berlin: Springer-Verlag, 1989.
24. P. G. Datskos, S. Rajic, and I. Datskou, "Photo-Induced Stress in Silicon Microcantilevers," *Appl. Phys. Lett.* **73**, 2319 (1998).
25. F. J. von Preissig, "Applicability of Classical Curvature-Stress Relation for Thin Films on Plate Substrates," *J. Appl. Phys.* **66**, 4262 (1989).
26. R. P. Feynman, R. B. Leighton, and M. Sands, *The Feynman Lectures on Physics*, vol. 2, 13th ed. Reading, MA: Addison-Wesley Publishing Company, 1964.
27. P. J. Shaver, "Bimetal Strip Hydrogen Gas Sensor," *Rev. Sci. Instrum.* **40**, 901 (1969).
28. P. I. Oden, E.A. Wachter, P.G. Datskos, T. Thundat, and R.J. Warmack, "Optical and Infrared Detection Using Microcantilevers," *SPIE - Infrared Technology XXII* **2744**, 345 (1996).
29. R. C. Weast, *Handbook of Chemistry and Physics*, 59th ed. Florida: CRC, 1972.